(3) *Ibid.*, **64**, 1166(1975).
(4) *Ibid.*, **65**, 231(1976).
(5) S. M. Beekman, U.S. pat. 3,208,906 (1965); through *Chem. Abstr.*, **63**, 17809a(1965).
(6) B. K. Davison and R. E. Schaffer, *J. Pharm. Pharmacol.*, **13**, 95T(1961).
(7) Y. Ideguchi and K. Shibata, Japanese pat. 7,005,659 (1970); through *Chem. Abstr.*, **72**, P103769y(1970).
(8) L. C. Greene, A. Misher, and W. E. Smith, U.S. pat. 3,591,680 (1971); through *Chem. Abstr.*, **75**, P80265b(1971).
(9) R. Persson and J. Sjoergren, German pat. 1,467,767 (1968); through *Chem. Abstr.*, **73**, P38544a(1970).

ACKNOWLEDGMENTS AND ADDRESSES

Received July 2, 1975, from the **Industrial and Physical Pharmacy Department, School of Pharmacy and Pharmacal Sciences, and the ‡Department of Agronomy, Purdue University, West Lafayette, IN 47907*

Accepted for publication October 23, 1975.

Supported in part by an American Foundation for Pharmaceutical Education Fellowship (S. L. Nail).

This report is Journal Paper 5945, Purdue University Agricultural Experiment Station, West Lafayette, IN 47907

ˣ To whom inquiries should be directed.

Kinetics and Mechanisms of Hydrolysis of 1,4-Benzodiazepines I: Chlordiazepoxide and Demoxepam

WESLEY W. HAN *, GERALD J. YAKATAN, and DALE D. MANESS ˣ

Abstract □ Differential absorbance spectroscopy was successfully used to follow the hydrolysis kinetics of chlordiazepoxide and demoxepam from pH 1 to 11. Loss of the methylamino group from chlordiazepoxide produced demoxepam. Demoxepam degraded by a parallel consecutive reaction to 2-amino-5-chlorobenzophenone and a glycine derivative. Two intermediates were observed by TLC for demoxepam hydrolysis. One was assigned the open-ring structure, resulting from amide hydrolysis, which kinetically appears to be the major mechanistic route leading to the benzophenone product. The other intermediate, representing an alternative but minor pathway, presumably results from initial scission of the azomethine linkage. Protonation of the *N*-oxide slightly alters the importance of these two pathways. Recyclization of the carboxylic acid intermediate was facile at pH values below the pKa of this intermediate. The stability parameters involving buffer catalysis, ionic strength effects, and temperature dependence of rate constants are reported.

Keyphrases □ 1,4-Benzodiazepines—kinetics and mechanisms of hydrolysis evaluated by differential absorbance spectroscopy □ Chlordiazepoxide—kinetics and mechanisms of hydrolysis evaluated by differential absorbance spectroscopy □ Demoxepam—kinetics and mechanisms of hydrolysis evaluated by differential absorbance spectroscopy □ Hydrolysis—chlordiazepoxide and demoxepam, kinetics and mechanisms, evaluated by differential absorbance spectroscopy □ Differential absorbance spectroscopy—evaluation of kinetics and mechanisms of hydrolysis of chlordiazepoxide and demoxepam

Little kinetic information is available on the solution stability and mechanisms of hydrolytic reactions of the 1,4-benzodiazepines. This class of nitrogen heterocycles is susceptible to acid–base-catalyzed hydrolysis at two potential sites of scission: the 1,2-amide linkage and the 4,5-azomethine bond. Both bonds undergo heterolysis under appropriate solvolytic conditions, forming a substituted benzophenone product and a glycine derivative (1–3).

Chlordiazepoxide (I) was reported (4) to degrade sequentially in aqueous solution, yielding 2-amino-5-chlorobenzophenone as the final product. An isolated intermediate in the reaction is the corresponding lactam, demoxepam (II); II is formed by hydrolytic cleavage of the methylamino substituent at the 2-position of chlordiazepoxide. That study (4) described kinetically the hydrolysis of chlordiazepoxide to the intermediate lactam. The purpose of the present study is to describe completely the kinetics and mechanism of hydrolysis from the parent molecule to the product benzophenone. This paper is the first of a series that will describe quantitatively the kinetics and mechanisms of hydrolysis of 1,4-benzodiazepines.

EXPERIMENTAL

Materials—The purity of the compounds was verified by TLC. Chlordiazepoxide[1], demoxepam[1], and 2-amino-5-chlorobenzophenone[1] were used without further purification. All other chemicals were of reagent grade quality. Distilled, deionized water was used for preparing aqueous solutions.

The buffer systems used were: pH 1.0–3.0, hydrochloric acid; pH 3.2–5.6, acetate; pH 4.7–7.4, phosphate; pH 6.9–9.5, borate; and pH 10.1–11, sodium hydroxide. The ionic strength was adjusted to 1.0 with sodium chloride, except for the ionic strength effect studies. The pH values were determined with a digital pH meter[2] at the temperature of the kinetic run.

Kinetic Measurements—The compound to be studied was dissolved in ethanol to make a 10^{-3} *M* stock solution. It was stored in the refrigerator in a light-protected flask to eliminate reported photolytic reactions (5). A light-protected reaction flask containing appropriate buffer solution was equilibrated at reaction temperature in a constant-temperature oil bath[3]. Less than ±0.05° variation was measured with an iron–constantan thermocouple.

An appropriate amount of stock solution was pipetted into the reaction flask so that the final concentration was about 10^{-5} *M*. An aliquot was withdrawn and quenched immediately in a light-protected ice water bath. The UV spectrum of the aliquot was measured as the zero-time sample on a recording spectrophotometer[4]. Subsequent aliquots were analyzed similarly at suitable time intervals for at least three half-lives of the slowest reaction. The final measurement, ab-

[1] Hoffmann–La Roche, Nutley, N.J.
[2] Orion model 701 equipped with a high temperature electrode, Cambridge, Mass.
[3] Sargent model SW equipped with a Sargent thermonitor (model ST), Dallas, Tex.
[4] Coleman model 124, Maywood, Ill.

sorbance at infinite time, was made after 10 half-lives. Beer's law plots were constructed to ensure that absorbance was directly proportional to concentration.

Product and Intermediate Identification—For isolation and identification studies, the solutions were prepared to be 10^{-3} *M*. Samples were withdrawn at various times, lyophilized, and redissolved in chloroform for TLC analysis. The chloroform solutions were spotted on silica gel GF plates, 250 μm, and eluted for about 50 min, using the solvent system of dioxane–benzene–hexane–7.4 *M* NH_4OH (45:50:70:5).

The chromatograms, after air drying, were visualized under UV light or developed with ninhydrin aerosol spray reagent. Reference standards, when available, were spotted directly on TLC plates. When possible, intermediates were isolated by preparative TLC (1000-μm plates). IR[5], NMR[6], and high-resolution mass[7] spectra were obtained on the isolated compound.

RESULTS AND DISCUSSION

Kinetically, the hydrolysis of 1,4-benzodiazepines may be expected to proceed as depicted in Scheme I. In this scheme, I represents chlordiazepoxide, II represents the 1,4-benzodiazepin-2-one, III is the intermediate resulting from hydrolysis of the 1,2-amide bond, IV is the intermediate derived from rupture of the 4,5-azomethine linkage, and V and VI are the products, benzophenone and the glycine derivative.

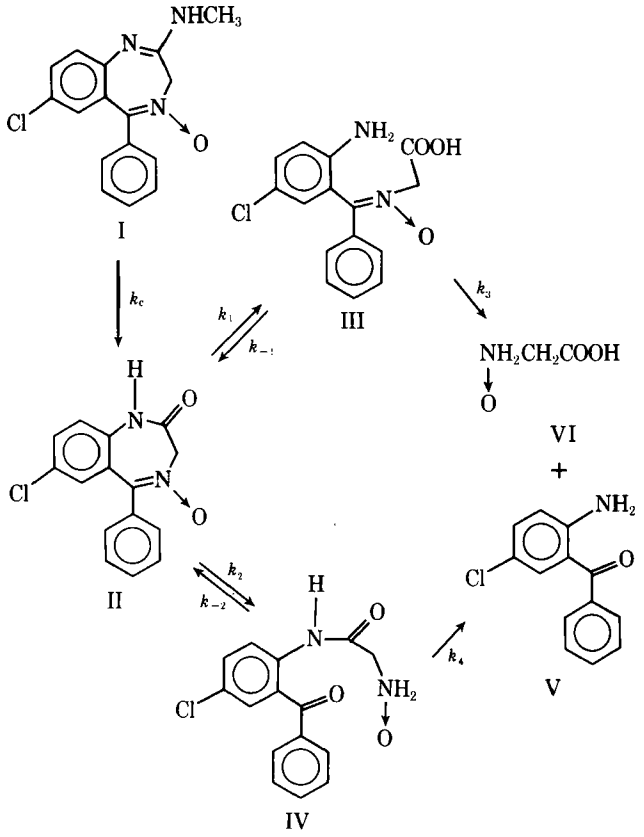

Scheme I

Chlordiazepoxide represents a special case of 1,4-benzodiazepine hydrolysis, since cleavage of the methylamino group is required to form II. Inclusion of this step adds an exponential term into a general integrated rate expression, but it can be experimentally eliminated by studying demoxepam hydrolysis. The two steps leading to intermediates III and IV are shown as reversible steps, since, under appropriate conditions, the reversion for III was experimentally observed (6). From entropy considerations, reversibility from final products to intermediates is not expected to be as favorable as the initial steps.

By solving the differential equations for Scheme I by using Laplace transforms and determinants, unique expressions for the concentration–time dependence of each species may be obtained:

$$[II]/[II]_0 = A_{11}\exp(-b_1t) + A_{12}\exp(-b_2t) + A_{13}\exp(-b_3t) + A_{14}\exp(-b_4t) \quad \text{(Eq. 1)}$$

$$[III]/[II]_0 = A_{21}\exp(-b_1t) + A_{22}\exp(-b_2t) + A_{23}\exp(-b_3t) + A_{24}\exp(-b_4t) \quad \text{(Eq. 2)}$$

$$[IV]/[II]_0 = A_{31}\exp(-b_1t) + A_{32}\exp(-b_2t) + A_{33}\exp(-b_3t) + A_{34}\exp(-b_4t) \quad \text{(Eq. 3)}$$

$$[V]/[II]_0 = A_{41}\exp(-b_1t) + A_{42}\exp(-b_2t) + A_{43}\exp(-b_3t) + A_{44}\exp(-b_4t) \quad \text{(Eq. 4)}$$

where [II], [III], [IV], and [V] are the molar concentrations of the species in Scheme I; $[II]_0$ is the initial concentration of II; and A_j and b_k are constants, which are related to combinations of the six rate constants given in Scheme I.

The absorbance at any wavelength and any time for the four-component system may be written as:

$$A = \epsilon_{II}[II] + \epsilon_{III}[III] + \epsilon_{IV}[IV] + \epsilon_{V}[V] \quad \text{(Eq. 5)}$$

where A is the absorbance, and ϵ_j is the absorptivity for species j. By combining Eqs. 1–5 and rearranging the terms, one obtains:

$$A_t - A_\infty = M\exp(-b_1t) + N\exp(-b_2t) + P\exp(-b_3t) + Q\exp(-b_4t) \quad \text{(Eq. 6)}$$

where A_t is the absorbance at any time; A_∞ is the absorbance at infinite time; and M, N, P, and Q are constants. Thus, ideally, a plot of logarithm of $A_t - A_\infty$ *versus* time should yield a tetraexponential curve with the slope of the last linear segment equal to the negative of the slowest rate constant. All other rate constants can be obtained by the feathering technique or by computer methods. Actually, the kinetics may be simplified by the competitive nature of the parallel sequential reactions. Thus, a tetraexponential curve may become a monoexponential, biexponential, or triexponential curve, depending on the magnitude of the rate constants and on the potential for reversibility of each reaction step.

For example, if the steps leading to intermediates are not reversible, Eq. 6 simplifies to:

$$A_t - A_\infty = M'\exp -(k_1 + k_2)t + N'\exp(-k_3t) + P'\exp(-k_4t) \quad \text{(Eq. 7)}$$

where the exponential factors are expressed in terms of the observed rate constants of Scheme I.

Spectral Changes and Rate Constant Determination—Spectral characteristics of the 1,4-benzodiazepines were described as superimposed spectra of two substituted benzene chromophores (7). This same report gave a pKa of 4.6 for chlordiazepoxide attributed to protonation of the *N*-oxide. Chlordiazepoxide spectral changes upon hydrolysis at pH values below the pKa showed two apparent reaction steps (Fig. 1). The first reaction step was characterized by an absorbance loss at 245 nm with a hypsochromic shift of λ_{max} from 245 to 236 nm. The second reaction was characterized by a loss in absorbance of both chromophoric absorption bands. Two new absorption bands with λ_{max} of 253 and 261 nm were observed.

The spectral changes for demoxepam in the same pH region were identical to the second reaction step of the hydrolysis of chlordiazepoxide. This finding indicated that the first observable reaction step of chlordiazepoxide was the formation of demoxepam, and the second reaction step was attributed to the ring-opening processes. The final product observed had the same spectrum as 2-amino-5-chlorobenzophenone. The benzophenone also exhibited an acid–base behavior, and its UV spectrum was dependent on the pH values. The end spectra of the hydrolysis of chlordiazepoxide at pH values close to the pKa of the benzophenone varied according to the spectral shifts observed with the benzophenone alone. The kinetic data were amenable to treatment according to the biexponential equation:

$$A_t - A_\infty = M\exp(-b_1t) + N\exp(-b_2t) \quad \text{(Eq. 8)}$$

Plots of the logarithm of $A_t - A_\infty$ *versus* time consisted of two linear segments. An isosbestic point at 270 nm was observed during the hydrolysis of demoxepam to benzophenone. By plotting absorbance

[5] Beckman model IR8, Fullerton, Calif.
[6] Joel model C60HL, Medford, Mass.
[7] Du Pont, CEC-21-110.

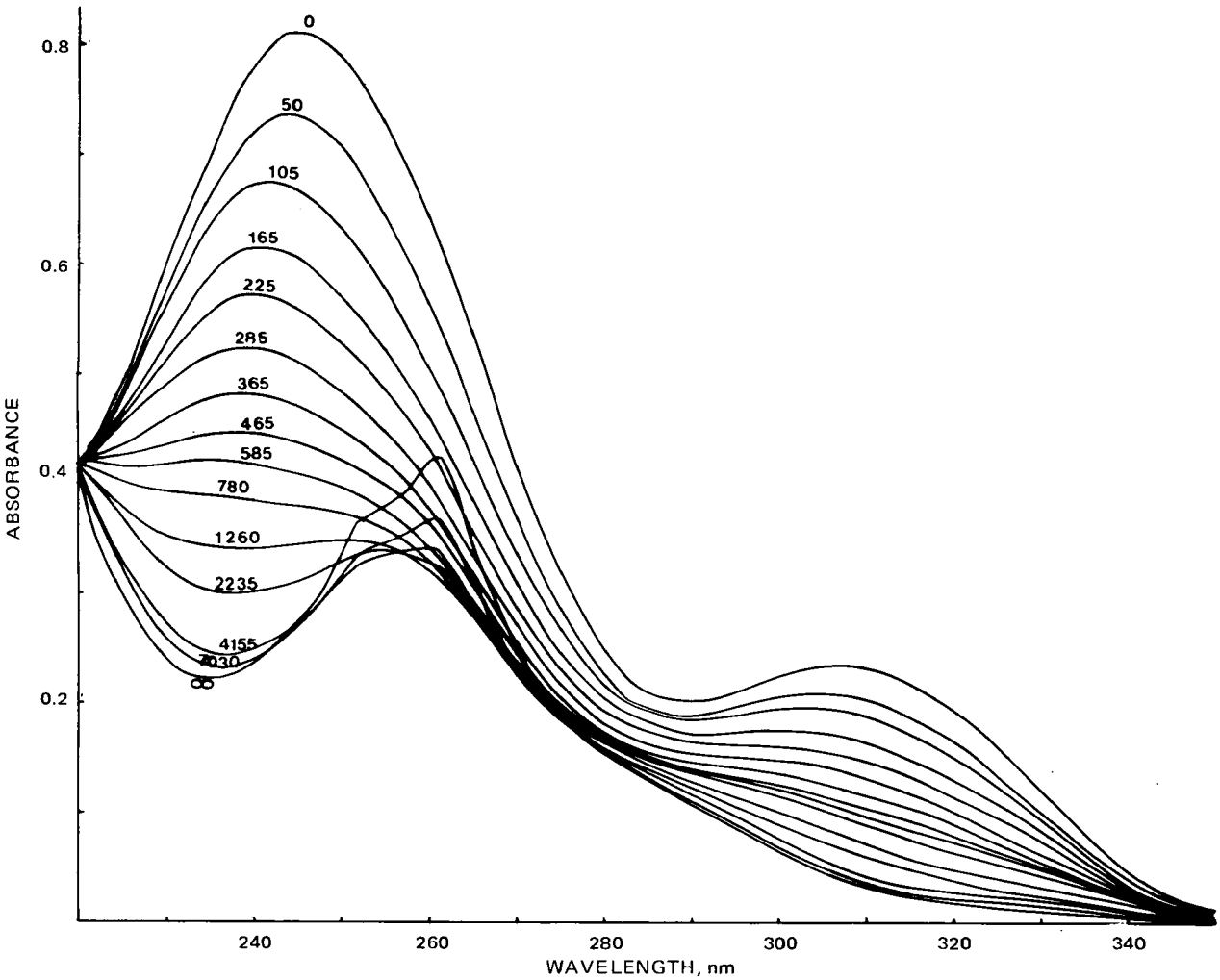

Figure 1—*Typical spectral changes for the hydrolysis of 10^{-5} M chlordiazepoxide in 0.1 N HCl, μ = 1.0, at 80°. Curves are labeled as to minutes after the start of the reaction.*

values at this wavelength, feathering to obtain the larger rate constant was unnecessary. Figure 2 shows a typical kinetic plot for the hydrolysis of chlordiazepoxide in 0.1 *N* HCl. Identical rate constants were obtained for the larger rate constant by employing either feathering or the isosbestic point plot. Both reaction steps demonstrated apparent first-order kinetics.

Table I—Apparent First-Order Rate Constants, $10^4 k$ (in Minutes^{-1}), for Chlordiazepoxide at 80°, μ = 1.0

pH	Buffer, *M*		k_c	k_1	k_3	r_c	r_1	r_3
		[HCl]						
0.93		0.1000	49.0	—	6.19	0.99	—	0.98
1.24		0.0398	20.6	—	—	0.99	—	—
1.70		0.0158	23.1	—	3.47	0.98	—	0.99
2.13		0.0063	23.9	—	—	0.90	—	—
2.60		0.0025	17.8	—	1.69	0.99	—	0.98
3.03		0.0010	22.7	—	—	0.99	—	—
	[CH_3COOH]	[CH_3COO^-]						
3.24	0.0957	0.0043	34.2	—	1.57	0.99	—	0.99
4.00	0.0761	0.0239	40.1	—	1.01	0.99	—	0.99
4.85	0.0322	0.0678	43.0	—	0.42	0.99	—	0.99
5.64	0.0081	0.0919	43.5	—	0.40	0.99	—	0.99
	[$H_2PO_4^-$]	[HPO_4^{-2}]						
4.73	0.0648	0.0018	43.0	—	0.52	0.99	—	0.99
5.58	0.0553	0.0011	47.7	—	0.28	0.99	—	0.99
6.47	0.0275	0.0391	48.2	11.80	0.20	0.99	0.97	0.97
7.40	0.0049	0.0617	44.3	21.00	0.24	0.99	0.99	0.99
	[H_3BO_3]	[$H_2BO_3^-$]						
6.96	0.103	0.003	31.0	—	—	0.97	—	—
7.93	0.103	0.029	41.4	2.70	0.32	0.99	0.98	0.99
8.52	0.061	0.112	39.9	5.88	—	0.99	0.98	—
9.53	0.003	0.100	39.9	31.32	0.31	0.99	0.99	0.99
		[NaOH]						
10.18		0.010	33.0	—	0.29	0.99	—	0.97
10.90		0.050	49.9	—	2.59	0.99	—	0.84

Table II—Apparent First-Order Rate Constants, $10^4\ k$ (in Minutes^{-1}), for Demoxepam at 80°, $\mu = 1.0$

pH	Buffer, *M*		k_1	k_3	r_1	r_3
		[HCl]	—	—	—	—
0.93		0.100	—	8.91	—	0.99
	[CH_3COOH]	[CH_3COO^-]	—	—	—	—
3.24	0.0957	0.0043	—	2.26	—	0.97
4.85	0.0322	0.0678	—	4.75	—	0.99
	[$H_2PO_4^-$]	[HPO_4^{-2}]	—	—	—	—
5.58	0.0553	0.0011	7.23	0.26	0.99	0.86
7.40	0.0049	0.0617	23.79	—	0.99	—
7.40	0.0049	0.0617	25.98	0.22	0.99	0.99
	[H_3BO_3]	[$H_2BO_3^-$]	—	—	—	—
6.96	0.103	0.003	—	0.25	—	0.98
7.93	0.103	0.029	2.96	0.28	0.99	0.99
8.52	0.061	0.112	7.60	—	0.99	—
9.53	0.003	0.100	49.60	0.34	0.99	0.99
		[NaOH]	—	—	—	—
10.18		0.010	250.16	0.30	0.99	0.95
10.90		0.05	>1000.00	3.60	—	0.98

The rate constants were calculated from least-squares analysis of slopes and are listed in Tables I and II for chlordiazepoxide and demoxepam, respectively. There was good agreement between the rate constants for demoxepam hydrolysis and the comparable rate constant for hydrolysis of the demoxepam derived from degradation of chlordiazepoxide, confirming that the first reaction step observed for chlordiazepoxide resulted in demoxepam formation. The last columns of each table give the correlation coefficients for the linear segments and suggest excellent linearity.

The spectral changes for chlordiazepoxide at pH values above the pKa of chlordiazepoxide and below pH 10 showed three apparent reaction steps. The initial spectral changes corresponded to the hydrolysis of the methylamino group at position 2. Spectral changes for hydrolysis of demoxepam in the same pH region were identical with the last two reaction steps of the hydrolysis of chlordiazepoxide. Above pH 10, the apparent first-order rate constant for the first step of hydrolysis of demoxepam was larger in magnitude than the apparent first step of the hydrolysis of chlordiazepoxide leading to demoxepam. Therefore, above pH 10, the reaction of demoxepam to the intermediate was not kinetically observed.

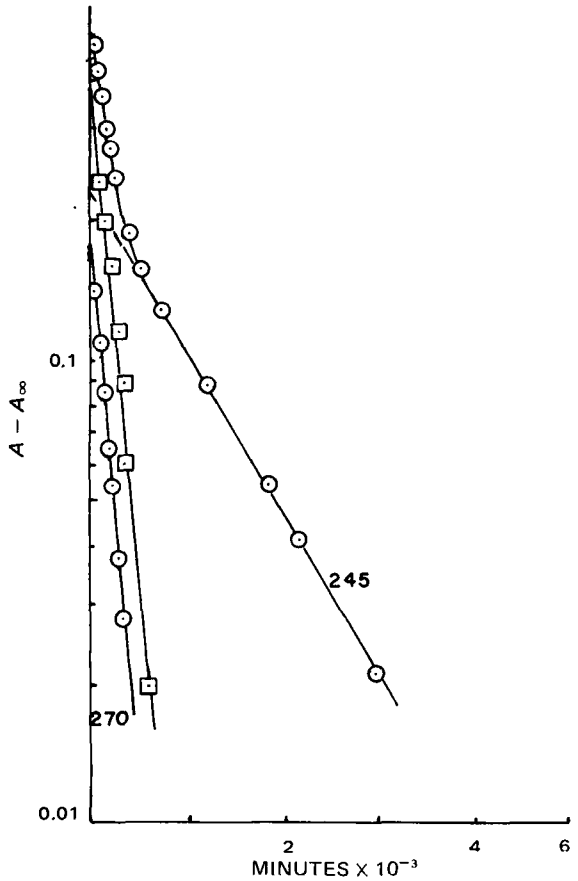

Figure 2—*Typical apparent first-order plots for hydrolysis of* 10^{-5} M *chlordiazepoxide in 0.1 N HCl, at 80°,* $\mu = 1.0$. *Plots are labeled as to wavelength;* □ *represents feathered data.*

Rate–pH Profiles—The log k–pH profile for hydrolysis of chlordiazepoxide to demoxepam (Fig. 3) was constructed from the logarithm of the apparent first-order rate constant, k_c, and pH values at 80° for ionic strength 1.0. In the acidic pH region, the rate–pH profile indicated hydrogen-ion catalysis on the protonated species. As the pH approached the pKa for chlordiazepoxide and more chlordiazepoxide existed in the neutral form, the observed rate constant became relatively independent of pH. This phase was attributed to water attack on the neutral species or hydroxide-ion attack on the protonated species as the kinetic equivalent.

As the pH values approached 2.5, the rate–pH profile indicated water attack on the protonated species or hydrogen-ion attack on the neutral species as the kinetic equivalent. This contribution to the overall log k–pH profile may be accounted for by:

$$k_{obs} = (k_H[H^+] + k_{H_2O} + k_{OH}[OH^-])f_{HS} \qquad \text{(Eq. 9)}$$

with the kinetic equivalents:

$$k_{H_2O}f_{HS} = k_{H'}[H^+]f_S \qquad \text{(Eq. 10)}$$

$$k_{OH}[OH^-]f_{HS} = k'_{H_2O}f_S \qquad \text{(Eq. 11)}$$

where f_{HS} and f_S are the fractions protonated and unprotonated, respectively.

The bimolecular rate constants were calculated according to Eq. 9 from the experimental data (Table III); the data were corrected for buffer catalysis. Based on these calculated values and the reported pKa at 80° for chlordiazepoxide, the fit of the theoretical curve to the experimental points is shown in Fig. 3. A reasonable fit was obtained, in good agreement with the data reported previously (4). This agreement suggests that the complex quantitative TLC method of analysis used in that study (4) is unnecessary.

The log k–pH profile for the second and third reaction steps for hydrolysis of chlordiazepoxide was constructed from the apparent

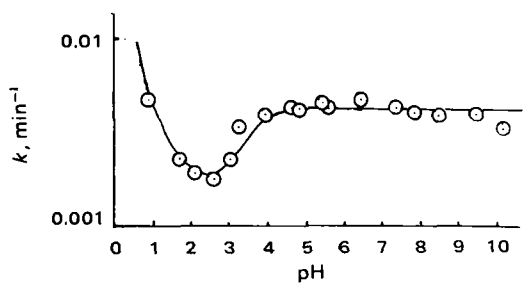

Figure 3—*Log* k–*pH profile for the hydrolysis of chlordiazepoxide at 80°,* $\mu = 1.0$, *first reaction step.*

Table III—Bimolecular Rate Constants (Minutes^{-1} M^{-1}) for Hydrolysis of Chlordiazepoxide and Demoxepam at 80°

k_H	k'_H	k_{H_2O}	k'_{H_2O}	k_{OH}	k'_{OH}	pKa
		Chlordiazepoxide, k_c				
0.03	—	0.0016	0.0045 (0.0036)[a]	—	—	4.6
		Chlordiazepoxide, Demoxepam, k_1				
—	—	—	—	6.1	—	—
		Chlordiazepoxide, Demoxepam, k_3				
0.0065	5.37	0.00017	0.000027	3640	0.014	4.2

[a] Corrected for buffer catalysis.

first-order rate constants, corrected for buffer catalysis, at 80° (Fig. 4). The data for hydrolysis of demoxepam also were plotted on the same graph. The two sets of data are in excellent agreement. The profile in the alkaline region indicates a two-step sequential reaction, both catalyzed by hydroxide ion on the neutral species. The log k–pH profiles in the acid region indicate hydrogen-ion catalysis on the positively charged ion, followed by water attack on the same species as the pH values increase. The observed apparent first-order rate constant for the acidic pH region can be described by:

$$k_{obs} = (k_H[H^+] + k_{H_2O} + k_{OH}[OH^-])f_{HS} \quad \text{(Eq. 12)}$$

The two possible kinetic equivalents are:

$$k_{H_2O}f_{HS} = k_H'[H^+]f_S \quad \text{(Eq. 13)}$$

$$k_{OH}[OH^-]f_{HS} = k_{H_2O}f_S \quad \text{(Eq. 14)}$$

Upon substitution of the dissociation constant, K_a, Eq. 11 becomes:

$$k_{obs} = (k_H[H^+] + k_{H_2O} + k_{OH}[OH^-])\frac{H^+}{H^+ + K_a} \quad \text{(Eq. 15)}$$

The values that produced the best fit are given in Table III. The kinetic pKa for the intermediate was calculated to be 4.2. The log k–pH profiles for the basic pH region can be represented for the first reaction step as:

$$k_{obs} = k_{OH}'[OH^-]f_S \quad \text{(Eq. 16)}$$

and for the second reaction step:

$$k_{obs} = k_{OH}[OH^-]f_S \quad \text{(Eq. 17)}$$

The values that provided the best fit are also given in Table III.

This interpretation of the rate–pH profiles for the second and third reaction steps provides a reasonably good fit to the experimental data over the 1–11 pH range. In spite of the possible complexity of the mechanistic scheme, the observed kinetic expressions are surprisingly simple. The specific rate constants calculated according to the profiles cannot be attributed to a unique kinetic step in Scheme I from these data alone. Therefore, examination by TLC of the reaction solution at reaction times when intermediates should be present was conducted.

Isolation and Identification—Samples withdrawn at appropriate times were subjected to TLC analysis as described under *Experimental.* Demoxepam (R_f 0.07) formation was observed from the hydrolysis of chlordiazepoxide throughout the entire pH range studied. The final products from hydrolysis of either chlordiazepoxide or demoxepam were 2-amino-5-chlorobenzophenone (visualized by short UV wavelength excitation) and the *N*-oxide glycine (purple spot produced at the origin upon spraying with 0.5% ninhydrin aerosol).

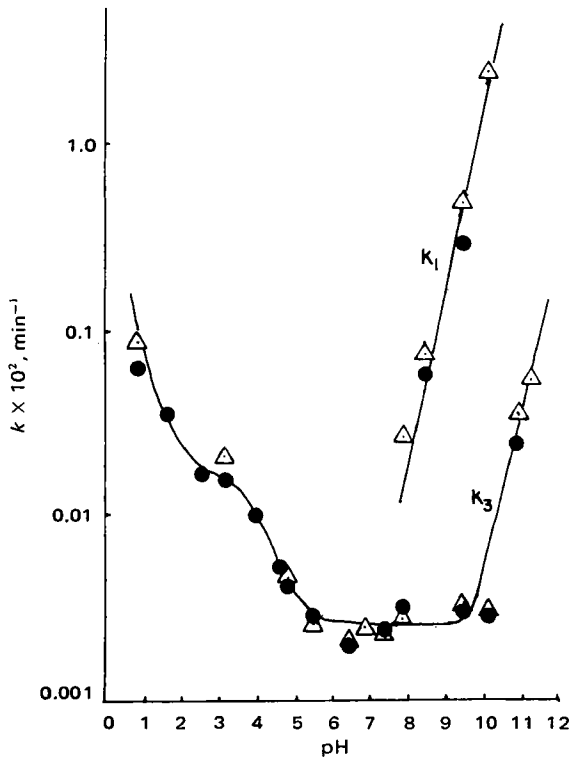

Figure 4—*Log* k–*pH profile for the hydrolysis of chlordiazepoxide and demoxepam at 80°, μ = 1.0. Key: ●, chlordiazepoxide; and △, demoxepam, second and third reaction steps.*

Subsequent to the appearance of demoxepam and prior to product formation, two other compounds were observed by TLC (R_f 0.27 and 0.43) and tentatively attributed to reaction intermediates IV and III, respectively. Visually, the intensity of these spots appeared to be similar at pH <5.0, although much less intense than the demoxepam spot. Above pH 5.0, the chromatograms showed two spots (R_f 0.0 and 0.27). The compound at the origin, upon acidification in pH 4.0 buffer and immediate TLC analysis, resulted in movement on the plate to an R_f value of 0.40. This finding implied that the compound at the origin is the conjugate base of intermediate III. In the basic region, the relative intensities of spots attributed to intermediates III and IV indicate that intermediate III formation is favored over the formation of IV. In fact, preparative TLC above pH 5.0 was successful in the isolation of III, whereas the small amount of IV formed precluded isolation.

Analysis by NMR and mass spectrometry did not prove useful in structure identification. Compound decomposition in the ionization chamber of the mass spectrometer was indicated by a color change in the compound from yellow to gray. The NMR spectrum showed only aromatic and methylene absorption, which would not differentiate between 1,2- and 4,5-bond scission. The IR spectrum of the potassium bromide disk did show a characteristic absorption peak for a carboxylic anion at 1610 cm^{-1}. Compound III was tentatively assigned the structure that would result from 1,2-bond cleavage. Sternbach and Reeder (2) and Bell *et al.* (6) reported the formation of the sodium salt of the carboxylic acid resulting from hydrolysis of the 1,2-amide linkage of demoxepam in alkaline solution, which supports this assignment.

Table IV—Apparent First-Order Rate Constants, 10^4 k (in Minutes^{-1}), for Hydrolysis of Chlordiazepoxide at Various Buffer Concentrations, μ = 1.0

pH	Buffer	Total Buffer Concentration as 1X	k_c 1X	2X	3X	4X	k_o	S[a]
4.74	$[CH_3COOH][CH_3COO^-]$	0.100	44.5	48.4	61.8	78.7	29	110
6.37	$[H_2PO_4^-][HPO_4^{-2}]$	0.066	44.4	50.5	51.3	55.4	38	51
8.55	$[H_3BO_3][H_2BO_3^-]$	0.173	38.3	37.1	35.6	—	—	—

[a] $S = k_{HA}[H^+]/K_a + k_A$.

Table V—Buffer Catalytic Constants for Hydrolysis of Chlordiazepoxide at 80°, $\mu = 1.0$

Buffer and pH	$10^4 k_{obs}$	$10^4 k_0$	$[A^-]$	$\frac{[k_{obs} - k_0]}{[A^-]}$	$\frac{[H^+]}{K_a}$	$10^4 k_{HA}$	$10^4 k_A$
$[CH_3COOH][CH_3COO^-]$							
3.24	34.2	18.0	0.00256	0.632	38.33	160	70
4.00	40.1	20.0	0.0133	0.153	6.66	—	—
4.85	43.0	30.1	0.0517	0.025	0.93	—	—
5.64	43.5	34.1	0.0868	0.012	0.14	—	—
$[H_2PO_4^-][HPO_4^{-2}]$							
4.73	43.0	28.0	0.000238	6.302	275.86	220	60
5.85	47.7	34.1	0.0030	0.456	20.92	—	—
6.47	48.2	36.0	0.011	0.110	5.01	—	—
7.40	44.3	36.0	0.041	0.019	0.58	—	—

Attempts to isolate sufficient quantities of III and IV below pH 5.0 were unsuccessful due to the small amounts present. It seems likely that IV is the ring-opened compound resulting from azomethine hydrolysis, although no confirming evidence is available to support this assignment.

Recyclization of Intermediate III—Subsequent to hydrolysis of demoxepam in basic solution leading to III, the reaction solution was acidified to pH 1. Maintenance of this solution at 24° resulted in spectral changes indicative of demoxepam formation. The apparent first-order rate constant for cyclization was 0.013 min^{-1}. This facile recyclization was not observed above pH 5.0, that is, in the pH region where III exists as the conjugate base. As the carboxylate anion, the carbonyl carbon would possess a smaller net positive charge, decreasing the possibility of nucleophilic attack of the aromatic amine. No recyclization above pH 5.0 was observed. Recyclization of IV was neither indicated nor discounted based on the experimental data.

Hydrolytic Mechanism—The preceding kinetic and TLC data are mechanistically interpretable in two separate pH regions: above and below the pKa values for demoxepam and the corresponding intermediates. Below pH 5.0, a monophasic first-order system is observed kinetically, even though TLC evidence demonstrated the presence of two intermediates, III and, presumably, IV. The observation of two intermediates implicates a parallel consecutive reaction, as depicted in Scheme I, with recyclization occurring for III (step k_1 reversible). At these pH values, the *N*-oxide would be protonated with strong resonance contribution from Structure VII.

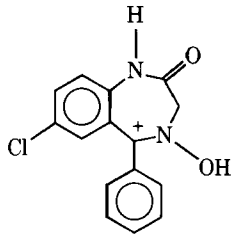

VII

Although models show that position 5 should be sterically hindered from nucleophilic attack, the resident positive charge due to protonation of the *N*-oxide must make attack at this position sufficiently competitive with nucleophilic attack on the carbonyl carbon so that IV is observable by TLC. The facile recyclization of III suggests that the 1,2-bond breakage is favored more than the TLC data would indicate. The monophasic behavior of the kinetic system infers that the predominant pathway for hydrolysis in this pH region proceeds through III as follows: II $\rightleftarrows$ III $\rightarrow$ V. Prior equilibrium for this system would result in:

$$\frac{A_t - A_\infty}{A_0 - A_\infty} = e^{-Kk_3 t} \qquad \text{(Eq. 18)}$$

with $K = k_1/k_{-1}$.

Table VI—Apparent First-Order Rate Constants, $10^4 k$ (in Minutes^{-1}), for Hydrolysis of Chlordiazepoxide at Various Ionic Strengths, 80°

pH	k_i	0.1	0.2	0.4	0.8	2Q
0.80	k_C	42.3	49.6	50.8	68.5	0.83
—	k_3	3.49	3.55	4.84	5.87	1.05

Other kinetic schemes with the inclusion of the relevant contribution from IV could be invoked but would necessitate numerous assumptions to transform the resulting tri- or tetraexponential equations into the observed monoexponential expression fitting the experimental data.

Above pH 5.0, the TLC data clearly indicate that formation of III is favored over IV. This preference is expected since the conjugate base of the protonated *N*-oxide group would not electronically favor nucleophilic attack at position 5. Additionally, since the complicating contribution from recyclization is absent, the simplified kinetic sequence in this pH region is: II $\rightarrow$ III $\rightarrow$ V. The operable equation for the biphasic system is:

$$A_t - A_\infty = Me^{-k_1 t} + Pe^{-k_3 t} \qquad \text{(Eq. 19)}$$

Thus, a simple nucleophilic attack on the amide linkage is followed by a similar nucleophilic reaction involving the azomethine linkage.

Stability Parameters—To provide a complete profile of the kinetic stability of chlordiazepoxide, hydrolysis kinetics as a function of buffer concentration, ionic strength, and temperature were investigated. Buffer catalysis was studied according to the relationship:

$$k_{obs} = k_0 + [k_{HA}[H^+]/K_a + k_A][A^-] \qquad \text{(Eq. 20)}$$

where K_a is the dissociation constant for the buffer species, k_0 is the hydrolysis rate constant in the absence of buffer catalysis, and k_{HA} and k_A are the rate constants for buffer catalysis of the acid buffer species and its conjugate base, respectively. Buffer effects were investigated by changing the original buffer concentration fourfold in a gradient manner. Table IV gives the results of these studies on the rate constant for transformation of chlordiazepoxide to demoxepam. Acetate and phosphate buffers catalyzed the hydrolysis, while borate had no effect. Table V presents the rate constants for the general catalysis observed with the acid and base species of both of these buffer systems. These values agree with those reported previously (4). Only phosphate catalysis was observed for the reaction of demoxepam to intermediate III. The buffer effect problem was avoided by changing to a different buffer system.

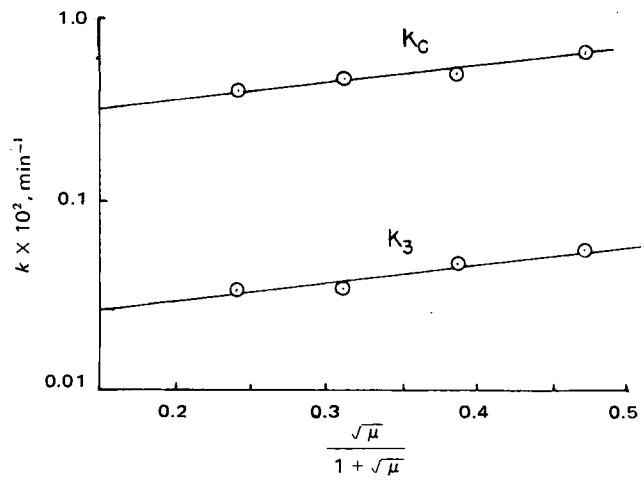

Figure 5—*Effect of varying ionic strength on apparent first-order rate constant for hydrolysis of chlordiazepoxide.*

Table VII—Apparent First-Order Rate Constants, 10^4k (in Minutes^{-1}), and Thermodynamic Parameters for Hydrolysis of Chlordiazepoxide

pH	k_i	85°	80°	75°	70°	E_a, kcal/mole	ln P	ΔH_a, kcal/mole	ΔS_a, cal/°K-mole
0.93	k_C	—	49.0	28.0	15.0	28.4	35.3	27.3	9.3
—	k_3	—	6.16	3.95	2.97	17.6	17.7	16.9	−25.6
11.23	k_3	8.01	—	5.47	2.37	18.4	18.8	17.5	−23.4

Ionic strength effects were observed for the biphasic hydrolysis of chlordiazepoxide at pH 0.80 (Table VI). Use of the Bronsted–Bjerrum equation together with the extended Debye–Huckel equation yields:

$$\log k = \log k_0 + 2QZ_AZ_B \sqrt{\mu}/(1 + \sqrt{\mu}) \qquad \text{(Eq. 21)}$$

where k is the apparent first-order rate constant, k_0 is the rate constant at zero ionic strength, Q is the constant equal to 0.55 at 80° (8), Z_A and Z_B are the charges of reaction molecules, and μ is the ionic strength. The positive slope values close to unity for the plots of log $k - \sqrt{\mu}/(1 + \sqrt{\mu})$ (Fig. 5) indicate that the reaction involves molecules of like univalent charge.

The apparent first-order rate constants were determined as a function of temperature in the strong acid and strong base regions. These values are given in Table VII along with the thermodynamic parameters obtained from slope and intercept values of the Arrhenius plots shown in Fig. 6. These values will allow stability prediction in the pH regions showing rapid degradation profiles.

CONCLUSIONS

A multicomponent solution resulting from a complex hydrolysis is often assumed not to be amenable to kinetic analysis by using absorbance spectroscopy. The present study demonstrated that this is not the case. Successful employment of absorbance spectroscopy yielded reasonably good kinetic data for the previously reported chlordiazepoxide to demoxepam reaction. Additionally, the parallel consecutive transformation of demoxepam to the benzophenone product was determined in the same manner without additional experimental workups such as extraction or TLC.

The hydrolysis of chlordiazepoxide to demoxepam may proceed uncatalyzed or by specific acid and base catalysis. This reaction step is subject to buffer catalysis with acetate and phosphate buffer systems. Ordinary ionic strength effects for bimolecular reactions involving like-charged molecules were observed only in the strong acid region.

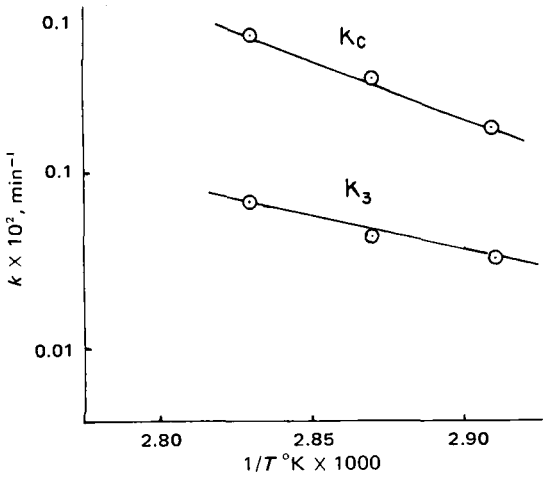

Figure 6—*Typical Arrhenius plots for apparent first-order rate constant for chlordiazepoxide, μ = 1.0.*

Further degradation of demoxepam involves ring opening to yield two intermediates, which subsequently are transformed into 2-amino-5-chlorobenzophenone and a glycine derivative. Throughout the pH region, the kinetically predominant intermediate is the one resulting from hydrolysis of the amide linkage. Initial hydrolysis of the azomethine bond is more competitive with the amide hydrolysis below pH 5.0. *N*-Oxide protonation below this pH electronically favors nucleophilic attack to compensate for adverse steric hindrance.

However, recyclization of the intermediate resulting from amide hydrolysis and the monophasic kinetics suggests that azomethine hydrolysis is still a minor pathway in the acid pH region. The log k–pH profile for demoxepam hydrolysis showed a specific base-catalyzed reaction. The transformation of the intermediate to the benzophenone product demonstrated specific acid- and base-catalyzed regions as well as an uncatalyzed hydrolysis. A kinetic pKa of 4.2 was calculated for intermediate III. Phosphate catalysis was observed for hydrolysis of III.

REFERENCES

(1) J. A. F. de Silva, *Anal. Chem.*, **36**, 2099(1964).

(2) L. H. Sternbach and E. Reeder, *J. Org. Chem.*, **26**, 4936(1961).

(3) J. T. Carstensen, K. S. E. Su, P. Madrell, J. B. Johnson, and H. N. Newmark, *Bull. Parenteral Drug Assoc.*, **25**, 193(1971).

(4) H. V. Maulding, J. P. Nazareno, J. E. Pearson, and A. F. Michaelis, *J. Pharm. Sci.*, **64**, 279(1975).

(5) L. H. Sternbach, B. A. Koechlin, and E. Reeder, *J. Org. Chem.*, **27**, 4671(1962).

(6) S. C. Bell, T. S. Sulrowski, C. Gochman, and S. T. Childress, *ibid.*, **27**, 562(1962).

(7) J. Barrett, W. F. Smyth, and I. E. Davidson, *J. Pharm. Pharmacol.*, **25**, 387(1973).

(8) J. T. Carstensen, *J. Pharm. Sci.*, **59**, 1140(1970).

ACKNOWLEDGMENTS AND ADDRESSES

Received September 2, 1975, from the *College of Pharmacy, University of Texas at Austin, Austin, TX 78712*

Accepted for publication October 29, 1975.

Presented in part at the Basic Pharmaceutics Section, APhA Academy of Pharmaceutical Sciences, San Francisco meeting, April 1975.

Abstracted in part from a dissertation submitted by W. W. Han to the University of Texas at Austin in partial fulfillment of the Doctor of Philosophy degree requirements.

Supported in part by a grant from the University Research Institute, University of Texas at Austin.

The authors express their gratitude to Dr. W. E. Scott of Hoffmann-La Roche Inc. for samples supplied and to Dr. Jay Nematollahi for helpful discussions.

* Present address: Searle Laboratories, Chicago, IL 60680

ˣ To whom inquiries should be directed.